Clay Minerals, (2014) **49**, 195–212

Weathering of volcanic ash in the cryogenic zone of Kamchatka, eastern Russia

E. KUZNETSOVA[1,*] AND R. MOTENKO[2]

[1] *SINTEF Building and Infrastructure, Trondheim, NO-7465, Norway, and* [2] *Lomonosov Moscow State University, Moscow, 119991, Russia*

(*Received 8 August 2012; revised 28 August 2013; Editor: Harry Shaw*)

ABSTRACT: The nature of the alteration of basaltic, andesitic and rhyolitic glass of Holocene and Pleistocene age and their physical and chemical environments have been investigated in the ash layers within the cryogenic soils associated with the volcanoes in the central depression of Kamchatka. One of the main factors controlling the alteration of the volcanic glass is their initial chemistry with those of andesitic (SiO_2 = 53–65 wt.%) and basaltic (SiO_2 < 53 wt.%) compositions being characterized by the presence of allophane, whereas volcanic glass of rhyolitic composition (SiO_2>65 wt.%) are characterized by opal. Variations in the age of eruption of individual ashes, the amount and nature of the soil water, the depth of the active annual freeze-thawing layer, the thermal conductivity of the weathering soils, do not play a controlling role in the type of weathering products of the ashes but may affect their rates of alteration.

KEYWORDS: volcanic ash, allophane, opal, unfrozen water, thermal conductivity, permafrost, Kamchatka.

The highly active volcanic area of Kamchatka in eastern Russia is part of the circum-Pacific belt of andesitic volcanism. It is situated north of the 49th parallel of latitude and is characterized by a severely cold climate with permafrost widespread above an altitude of 700 m. The Kamchatka peninsula is blanketed by a soil-pyroclastic cover (Melekestsev *et al.*, 1969) consisting of loose, pyroclastic material from explosive eruptions and buried soil beds. Ashes from major eruptions form clear marker horizons and can be traced over wide areas. This has allowed a well defined tephro-stratigraphy to be established that is based upon the chemical signature of the glass (Braitseva *et al.*, 1997). Between the key ash marker horizons are other pyroclastic deposits derived from both minor local and remote eruptions and from the secondary re-deposition of ash (Bazanova *et al.*, 2005).

Considerable research has been carried out on the weathering of volcanic glass. For volcanic ash soils in warm humid climates Wada & Wada (1977) suggested that the sequence of weathering is volcanic glass → allophane → halloysite or volcanic glass → opal → allophane → halloysite. For the rhyolitic glass in the humid conditions in Japan, the allophane → halloysite transformation occurs after 6000 years (Wada & Wada, 1977; Nagasawa, 1978; Wada, 1989). However, other studies have shown that, depending on their different glass compositions, volcanic ash may weather directly to halloysite as well as to allophane (Parfitt *et al.*, 1983; Parfitt & Wilson, 1985). Basaltic glass (SiO_2:Al_2O_3 < 4) has an intrinsically smaller molar Si:Al ratio and a soft and porous structure that favours weathering at a much higher rate than rhyolitic glass (SiO_2:Al_2O_3 = 5 to 6) (Lowe, 1986).

* E-mail: elena.kuznetsova@sintef.no
DOI: 10.1180/claymin.2014.049.2.04

The influence of climatic variation on the weathering of volcanic glass is still to be clarified, particularly in the extremely cold climates associated with high precipitation. In this paper we report on our study of the breakdown of volcanic glass in the soil-pyroclastic cover associated with the Klyuchevskaya group of volcanoes situated in the Central Depression of Kamchatka (55–56ºN, 160–161ºE). The group consists of several active volcanoes (Klyuchevskoy (~4800 m), Bezymianny (~2900 m), Ushkovsky (~3900 m), Plosky Tolbachik (~3100 m) plus ten others that are not active today, together with numerous small cinder cones, extrusive domes and other volcanic features (Braitseva *et al.*, 1995). It is the location where the Large Fissure Tolbachik Eruption took place in 1975 and 1976, during which about 500 km^2 were covered by scoria and ash and 3 new cinder cones and lava fields were formed (Fedotov & Markhinin, 1983).

The climate of the study area is characterized by cold winters, as well as mild and wet summers that are mainly influenced by cyclonic activity. No permanent meteorological station exists in the mountainous areas, but the Klyuchi station (WMO 32389), situated in the Kamchatka river valley at an elevation of 29 m and about 30–40 km from the central part of volcanic area, provides a long-term climatic record for the region. The mean annual average temperature in Klyuchi is −0.7ºC for 1910–2007 and ~0ºC for 1970–2007. The total annual precipitation in Klyuchi is ~500 mm, whereas in the mountains it is estimated to be ~1000 mm (Muravyev, 1999). In Klyuchi the snow cover usually lasts from October to June with a snow cover thickness of ~1.5–3 m in forested areas and 50–80 cm or less in open areas due to redistribution by strong winds (Abramov *et al.*, 2008).

Permafrost and periglacial processes are widespread. The lower boundary of the permafrost is at 750–900 m above sea level for the northern slopes and 650–800 m for the southern ones. Numerous solifluction lobes, clay cryoturbation spots, polygonal structures, and areas of sorted ground occur between altitudes of 1000 and 1700 m. The thickness of the seasonal freezing-thawing active layer decreases with increasing altitude and may vary slightly from year to year. The maximum seasonal melting of permafrost is up to 2.5 m at 900 m and 50 cm at 2500 m (Abramov *et al.*, 2008).

There are from six to eight soil profiles developed in the soil-pyroclastic cover associated with these volcanoes. In each there is an organic horizon that overlies volcanic ash. The soils have a small humus content ~ 1 to 2.4%, which is not typical for most volcanic soils of Kamchatka (Zakharikhina, 2009); this reflects the interplay of permafrost, relatively low rainfall and the abundant deposition of airborne volcanic material.

ANALYTICAL METHODS.

A total of 24 samples (Table 1) were collected at elevations between 130 and 1630 m. Samples *1-6* were collected from the active layer in the thawed state, sample *7* in the frozen state from a depth of 2.50 m in a drill hole and other samples from the frozen active layer.

The moisture content (ratio of the mass of water to the mass of dry sample) was determined by drying the wet samples at 105ºC for 12 h. Adsorbed water was determined by drying samples to constant weight from room temperature to 105ºC.

Thermal studies (TG, DTG, DTA analyses) were carried out using a Q-1500D derivatograph over the range from room temperature to 1000ºC with a heating rate of 20ºC/min (Topor *et al.*, 1987). The loss of absorbed (low) water over the range from room temperature to 110ºC was observed on the heating curves of the samples (*3*, *4*, *8*, *9*, *13*, *15*, *17*, *24*), and the endothermic effects recorded over the range from 110 to 750ºC corresponded to the loss of structural (high) water by the ash material. The total mass loss (structural water + absorbed water) is designated as W_{term} and its values are shown in Table 6.

From the weight difference between the wet and dried sample and the volumes of the sample, the dry bulk density and water content were calculated. Solid particle density (mineral density of rock) was measured for rock powder on an exclusive device ELA (Kalachev *et al.*, 1997). The underlying principle of this device is the law of Boil-Moriotte (pressure × volume = constant in an isothermal environment); the accuracy is 0.02 g/cm^3.

Particle-size distribution patterns were determined for most samples by a combination of sieving and the pipette method after dispersion with sodium hexametaphosphate.

Chemical analysis was restricted to several representative samples based on their similar stratigraphical positions in comparative marker

https://doi.org/10.1180/claymin.2014.049.2.04 Published online by Cambridge University Press

TABLE 1. Location, volcanic source, age and physical characteristics of the ash samples.

Sample no.	Sampling point	Source volcano	Tephra index	Height (m)	Depth (m)	Mean age, ^{14}C years	Moisture content W (%)	Absorbed moisture W_g (%)	Dry density, ρ_d, (g/cm^3)	Solid particles density, ρ_s (g/cm^3)
1	Tolbachinskiy Pass	–*	–*	1630	0.2	1500	38	2.04	1.1	2.69
3					0.55	1500	64	4.3	0.9	2.70
5					0.75	1500	31	1.67	1.3	2.73
7					2.5	1500	30	1.24	1.5	2.80
2	Near Large Fissure Tolbachik Eruption cones (LFTE)	Tolbachik	–*	1330	0.2	35	21	0.3	1.1	2.52
8					0.5	35	–*	–*	–*	–*
4	Cones in the Kamen Volcano area	–*	–*	1000	0.15	ND	21	0	1.3	2.64
6					0.4	ND	13	0.2	1.5	2.71
9	Moraine complex of the Bilchinok glacier, right slope of the bold mountain	Khangar	Khg	695	0.36	6850	42	1.32	0.9	2.47
10		–*	–*		0.56	~7500	37	1.94	1.3	2.79
11	Moraine complex, right slope of the Bilchinok glacier valley	Shiveluch	Sh_2	746	0.45	950	32	0.46	1.1	2.66
12			Sh_3		0.70	1400	36	0.81	1.1	2.61
13			Sh_5		1.2	2550	32	1.0	1.1	2.52
14	Left slope of the Bilchinok glacier valley, at the forest boundary	–*	–*	290	1.15	~6000	34	3.94	0.9	2.79
15		Khangar	Khg		1.32	6850	36	2.52	0.8	–
16		–*	–*		1.5	6850–8300	42	4.14	0.9	2.1
17		Shiveluch	Sh_{8300}		1.71	8300	11	1.67	1.0	2.71
18		–*	–*		1.8	~9000	69	7.3	0.8	2.46
19	Seismic station on Podkova, Klyuchevskoy volcano slope	Shiveluch	Sh_2	800	0.65	950	32	0.3	1.0	2.68
20		Klyuchevskoy	–*		0.85	950–400	31	0.79	1.1	2.75
21					1.17		30	0.87	0.9	2.74
22	Nappe Apakhonchich	Shiveluch	Sh_2	800	1.1	950	43	0.32	1.5	2.58
23		Ksudach	KS-1		2.2	1800	51	0.56	1.1	2.68
24	Kamchatka river valley, steep bank 'Krutoy"	–*	–*	130	5.2	Q_1^2	–*	0.93	–*	2.45

* the specified volcanic ashes do not form key beds because they are the products of minor or remote eruptions. Consequently, they cannot be referred to a particular source volcano or a particular tephra index.

layers (e.g. between layer Sh_2 and Sh_3) or in relation to existing published data.

The chemical compositions of the volcanic ash samples *1–7*, *14*, *15* and *22–24* were determined by wet chemical analyses in the chemical laboratory of the Petrology Department of Moscow State University. SiO_2 and H_2O were determined gravimetrically; CaO, MgO, Al_2O_3, TiO_2 and Fe_2O_3, complexometrically; and Na_2O and K_2O by flame photometry (Jeffery & Hutchison, 1983).

The salinity of the soil water was determined using a salinometer based on electrical conductivity (EC) measurements of soil-water extract.

The mineral composition of the ashes was determined by infrared absorption spectroscopy using a LOMO FSM-1201 infrared Fourier spectrometer. The absorption spectra were recorded over the range from 400 to 4000 cm^{-1} at room temperature with an accuracy of frequency determination of ±1 cm^{-1}. The samples were prepared using two procedures: powdered samples (2 mg per 250 mg of KBr) were pressed into transparent tablets, or as suspensions in petroleum oil (Plyusnina, 1977). Interpretation of the spectra was made by comparison with standard mineral spectra published by Peng Wenshi (1982). SEM images of the samples and chemical composition of the volcanic glass and some minerals were obtained at the Petrology Department of Moscow State University by EPMA using a Jeol JSM-6480LV instrument with an INCA-Energy 350 spectrometer for compositional analysis. The samples were prepared as polished thin sections and SEM images presented in this paper are backscatter images.

Transmission Electron Microscopy (TEM) analysis was performed in the NTNU/SINTEF Gemini Centre using a JEOL 2010F instrument equipped with an Oxford Instruments SDD X-ray detector for chemical analysis. Samples were prepared by first dispersing a small sample of ash in propanol in a glass vial, assisted by placing the suspension in an ultrasonic bath. A significant proportion of the ash settled within a few seconds. A drop of the remaining suspension, expected to contain a higher proportion of the smaller component particles, was placed onto a perforated carbon film supported on a standard Cu-mesh TEM grid and allowed to dry before examination.

Samples *1–7* were radiocarbon dated at the laboratory of the Department of Geography, University of Zurich (GIUZ) using AMS (accelerator mass spectrometry) with a tandem accelerator at the Institute of Particle Physics based at the Swiss Federal Institute of Technology Zurich (ETH).

The dating of other samples was made by comparison to the well established scheme of tephrochronology developed for Kamchatka and based on a combination of the varying chemistry of the marker ash layers and radiocarbon dating of the organic soils, combined in sample *24* with pollen and diatom analysis (Braitseva *et al.*, 1968). Marker ashes are dated and have their own index accompanied by a number or letter. For example, the tephra of the Shiveluch volcano from eruption 'Sh_2' are 950 years old, from eruption 'Sh_3' – 1400 years, from eruption 'Sh_5' – 2550 years, and from eruption 'Sh_{8300}' – 8300 years. The Khangar volcano tephra horizon with the index 'Khg' are 6850 years old, and the Ksudach volcano ashes with the index 'KS_1' are 1800 years old (Ponomareva *et al.*, 2007a, b). The dating of the samples between marker layers was made by calculation.

Determinative methods for thermal properties and unfrozen water content in frozen and thawed grounds are described in Motenko & Kuznetsova (2009a), Kuznetsova *et al*. (2011) and Kuznetsova & Motenko (2011b, 2012).

RESULTS

Sample ages

The ashes are mainly of Holocene age (0–12000 years), the only exception being sample *24* which has been dated by its sporo-pollen and diatom assemblages as belonging to the upper part of the early Pleistocene (Q_1^2) (Braitseva *et al.*, 1968) (Table1).

Physical properties

The physical properties of the soils are summarized in Table 1. The water contents range from 13 to 69%, the adsorbed water ranges from 0 to 7.3%, the dry density from 0.9 to 1.6 g/cm^3 and the solid particle density from 2.1 to 2.8 g/cm^3. Particle size distribution showed that nearly all the ashes are of fine sand size. The predominant fraction in most samples is 0.1–0.05 mm, although for samples *2–4* it is 0.05–0.01 mm, for sample *17* it is 0.25–0.1 mm and sample *24* is predominantly of silt size with 60% of its total being less than 56 μm

https://doi.org/10.1180/claymin.2014.049.2.04 Published online by Cambridge University Press

(Kiryanov, 1981). The particle size limits applied for sand, silt and clay are based on standard procedures used in Russia, but these are similar to those used in Europe and USA.

Chemical properties

The major primary components in fresh tephras include volcanic glass, plagioclase and pyroxenes as well as other minerals (Nanzyo, 2002). The most abundant component is glass which can be divided into noncoloured and coloured varieties. Rhyolitic, dacitic and andesitic tephras contain non-coloured volcanic glass while basaltic tephra contains coloured volcanic glass (Yamada & Shoji, 1983).

The chemical compositions of ash and volcanic glass in several samples are shown in Tables 2 and 3. In addition reference is also made to chemical data for ash and glass samples used in this study that have previously been published by Braitseva *et al.* (1997) and Ponomareva *et al.* (2007a,b). The volcanic glasses are generally either andesitic (SiO_2 < 65%) or rhyolititic (SiO_2 > 65%), although the glass from samples *8*, *20* and *21* is basaltic (SiO_2 < 53%) (Braitseva *et al.*, 1997). The bulk composition of the fresh tephra reflects the overall bulk chemical composition of its mineral and glass components and not necessarily the composition of the glass components. For example, combinations of andesitic ash with rhyolitic glass or basaltic ash with andesitic glass are not uncommon.

The soil water salinity measurements indicate that all ashes, except sample *24*, have low salinities; their total soluble salt content is about 0.02–0.03%. Sample *24* has a high salinity, the total soluble salt content is 1.815 % and the main component is sulfate (SO_4^{2-} 1.242%). The hydrochloric acid extract from this sample shows that the content of SO_4^{2-} is 0.47%, and Fe^{2+} 0.44%. Assuming that Ca^{2+} is associated with the sulfate ion, the content of $CaSO_4$ is 0.67%. The pH of this saline water sample was 3.4 (Table 4).

The organic carbon content of the samples range from 0 to 0.03 wt.%.

Infra-red analyses

Yamada & Shoji (1975) found that the composition of tephra is dependent on particle size; the mineral content tends to be high in the fraction coarser than 0.1 mm in diameter, whereas volcanic glass tends to be abundant in the <0.1 mm fraction.

TABLE 2. Chemical composition (wt.%) of some ash samples.

Sample no.	SiO_2	Al_2O_3	FeO	Fe_2O_3	TiO_2	P_2O_5	CaO	MgO	MnO	Na_2O	K_2O	H_2O	LOI	Total
1	52.75	19.04	2.59	4.84	1.24	0.52	6.65	2.77	0.13	2.49	1.45	0.66	4.04	99.18
2	63.59	14.88	1.44	3.18	0.55	0.21	4.55	3.65	0.09	3.3	1.69	0.12	1.38	98.63
3	53.05	19.03	2.87	4.37	1.43	0.64	4.55	1.64	0.12	2.8	2.05	2.28	4.7	99.53
4	60.86	16.62	1.44	5.42	0.73	0.15	6.48	3.53	0.14	2.9	1.27	0.1	0.36	100.0
5	55.12	19.03	2.95	4.15	1.24	0.61	6.83	2.77	0.11	2.9	1.72	0.38	2.26	100.07
6	58.31	16.79	1.94	5.16	0.73	0.15	7.35	4.41	0.14	2.77	1.11	H.o.	0.52	99.38
7	52.11	16.45	3.45	4.56	1.01	0.21	7.88	5.53	0.15	2.57	0.84	0.34	3.86	98.96
14	49.34	17.44	3.66	5.15	1.01	0.17	7.88	6.55	0.15	2.16	0.63	1.64	4.26	100.04
15	61.82	16.06	1.00	2.77	0.54	0.09	2.98	1.51	0.09	3.1	1.99	1.74	5.98	99.67
22	52.7	18.29	2.37	5.85	1.01	0.19	8.75	4.03	0.14	2.66	0.66	0.50	2.2	99.35
23	66.64	15.53	2.01	2.17	0.48	1.10	3.15	1.26	0.14	3.54	0.99	0.36	2.88	100.25
24	66.89	13.78	–	3.27	0.28	0.10	2.45	0.50	0.06	3.07	2.59	1.00	5.5	99.49

LOI: loss on ignition

https://doi.org/10.1180/claymin.2014.049.2.04 Published online by Cambridge University Press

TABLE 3. Chemical composition (wt.%) of volcanic glass in some samples, obtained by EPMA.

Sample no.	SiO_2	Al_2O_3	FeO	TiO_2	P_2O_5	CaO	MgO	MnO	Na_2O	K_2O
1	60.6	15.4	7.5	–	1.6	0.8	5.02	2.3	–	3.7
3	62.9	16.17	6.04	1.2	0.48	4.13	1.76	–	4.11	3.21
5	53.08	15.67	10.57	–	1.9	0.8	7.61	4.21	0.3	3.52
7	53.9	15.7	10.3	1.8	0.7	7.6	3.9	0.1	3.6	2.4
14	58.4	24.2	2.16	–	0.36	0.36	8.85	0.37	–	4.8
18	64.4	14.8	7.27	0.03	0.81	4.11	1.72	0.1	2.93	3.84
2	77.72	13.7	1.11	–	–	–	1.1	0.25	–	3
4	77.7	11.9	1.8	0.6	0.2	0.7	0.2	–	2.2	4.7
6	77.32	11.4	1.3	–	–	–	0.3	2.72	–	1.62
9	77.7	13.7	1.29	0.11	–	1.3	0.27	–	2.4	3.3
12	77.94	13.86	1.25	–	0.3	–	1.2	0.31	–	2.22
13	78.2	13.9	1.09	0.35	–	1.16	0.25	–	2.08	2.9
15	78.3	13.5	1.14	0.05	0.07	1.24	0.35	–	2.17	3.3
17	77.5	14.1	1.26	–	0.3	–	1.32	0.27	–	2.3
*24**	72.27	13.87	1.54	0.44	1.37	2.89	0.63	0.07	3.85	3.07

* data from Kiryanov (1981)

Infra-red analysis was carried out therefore on the volcanic glass-rich fine fraction (<0.1 mm size fraction) of the tephra.

Peng Wenshi (1982) showed that the typical frequency of the Si–O absorption bands for opal occur at 472, 790 and 1100 cm^{-1}, and for allophane at 430, 575 and 965 cm^{-1}.

The IR absorption spectra from samples of the glass samples are shown in Fig. 1. The spectrum from sample *2* indicates the presence of "anhydrous opal" (bands at 446, 786 and 1080 cm^{-1}), whereas the spectra from samples *9* (*15*), *13*, *32* (Fig. 1b,c,d), indicate opal ($SiO_2 \cdot nH_2O$) with a varying water content. The Si–O absorption bands occur at 465–471, 781, 1050–1060 cm^{-1}. The spectrum shown in Fig. 1e is for sample *8* (35 years old) which is essentially an aluminosilicate glass containing "anhydrous allophane" (IR absorption bands at 440, 553 and 987 cm^{-1}), whereas samples *3*, *7*, *18* and *20* (Fig. 1f,g,h,i) contain allophane ($mSiO_2 \cdot kAl_2O_3 \cdot nH_2O$) (Si–O absorption bands at 434–457, 565–567, 980–995 cm^{-1}).

TABLE 4. Results of chemical analyses of ash water extracts (based on 100 g of dry sample). pH = 3.4

Elements	mg·eq %	% w/w
Cl^-	–	–
HCO_3^-	–	–
SO_4^{2-}	25.84	1.241
NO^{2-}	–	–
NO^{3-}	0.29	0.018
NH^{4+}	2.16	0.039
Ca^{2+}	1.00	0.020
Mg^{2+}	2.25	0.027
Fe^{2+}	3.15	0.088
Fe^{3+}	5.06	0.094
*Na^+	12.52	0.288
Σ salts	— 1.815 % w/w —	

The occurrence of water in the form of molecular H_2O was identified by the band near 1630 cm^{-1} in the IR absorption spectra. This corresponds to deformation vibrations (vibrations with angular alterations) of the H_2O molecule, and the simultaneous presence of a broad absorption band at 3100–3700 cm^{-1} in the spectra related to valence vibrations on O–H bonds. An increase in water content for each glass type was observed in the IR absorption spectra with increasing age of the ash. The absorption spectra also demonstrated the presence of traces of crystalline phases which we were unable to identify in our investigation.

Comparing IR results with glass composition indicates that allophane is associated with andesitic and basaltic glass, and opal with rhyolitic glass.

SEM and TEM analyses

Allophane. Backscatter electron micrographs from SEM analyses are shown in the Figs 2 and 3.

https://doi.org/10.1180/claymin.2014.049.2.04 Published online by Cambridge University Press

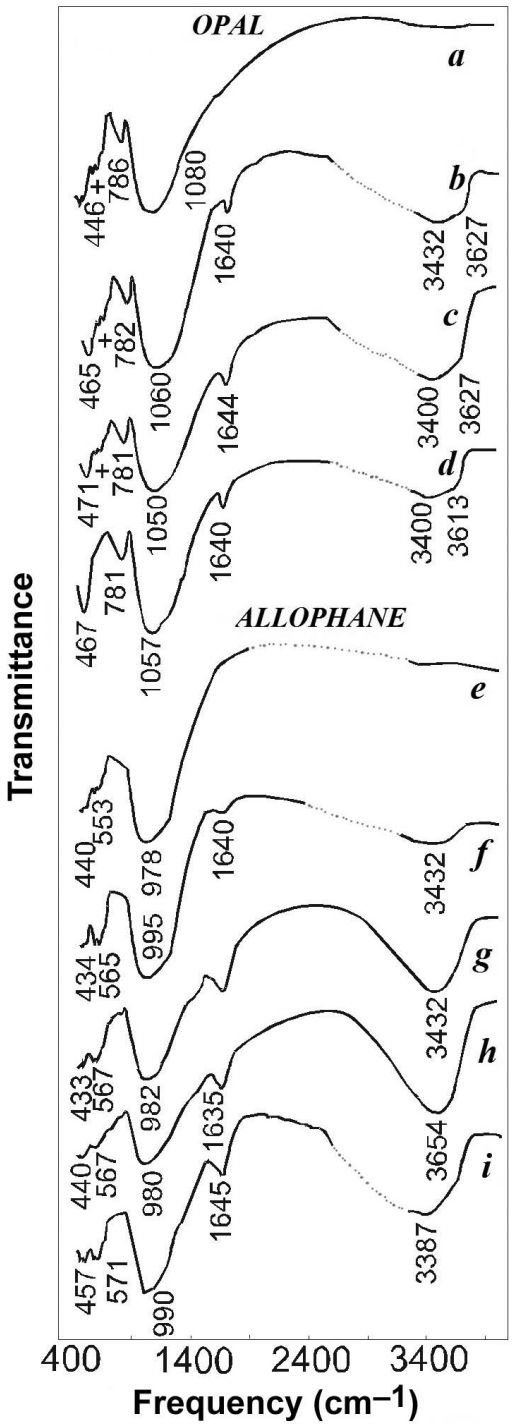

FIG. 1. IR spectra of ashes studied: (a) Amorphous silicate ("anhydrous opal") in sample *2*, age 35 years (in KBr pellet); (b) Opal in sample *13*, age 2500 years (suspension in vaseline oil); (c) Opal in samples *9* and *15*, age 7000 years (suspension in vaseline oil); (d) Opal in sample *32*, early Pleistocene (Q_I^2) (suspension in vaseline oil); (e) Predominantly alumosilicate glass ("anhydrous allophane") in sample *8*, age 35 years (suspension in vaseline oil); (f) Allophane in sample *20*, age 950–1400 years (suspension in vaseline oil); (g) Allophane in sample *7*, age 1500 years (in KBr pellet); (h) Allophane in sample *3*, age 1500 years (in KBr pellet); (i) Allophane in sample *18*, age 9000 years (suspension in vaseline oil).

Figure 2 shows the image of a glass particle with an alteration rim that has been interpreted as allophane. The accompanying elemental distribution maps suggest a relative enrichment of Fe and Al in the allophane coating accompanied by desilicification of the glass and possible leaching of Mg, Na, K and Ca along the contact with the allophane.

Figure 3 shows backscatter images of two ash samples; no. *5* – 1500 years old (Fig. 3a) and no. *18* – 9000 years old (Fig. 3b). In the younger sample with less weathering, allophane forms a rim along the contact between vesicles and glass, but in the older sample with greater age and weathering, the leaching and desilicification of glass has resulted in very fine-grained mixtures of short-range-order aluminosilicates (allophane) (Fig. 3*b*), with Al/Si ratios of ~ 1.4–1.6 (Table 5, *A1* and *A2*).

Opaline silica. Opaline silica was present as very fine particles and these could only be seen clearly at high magnification using transmission electron microscopy. TEM micrographs of sample *24* are shown in the Figs 4–6. There is some evidence that the opaline silica particles are spherical in form and are closely packed in microaggregates (Fig. 4a and b), as described by Shoji & Masui (1971) and by Pollard & Weaver (1973). The forces and processes involved in the aggregation of the particles are not entirely understood, but there are suggestions that the long-range electrostatic repulsion force, that is between similarly charged objects, and the short-range van der Waal's forces are the major forces that predetermined the configuration of the aggregate made up of silica spheres (Deveson, 2004). The opaline silica particles are extremely thin; the size of each particle can be up to 10–20 nm.

Figure 5a shows a corroded edge of the opaline silica which suggests that dissolution occurs during

https://doi.org/10.1180/claymin.2014.049.2.04 Published online by Cambridge University Press

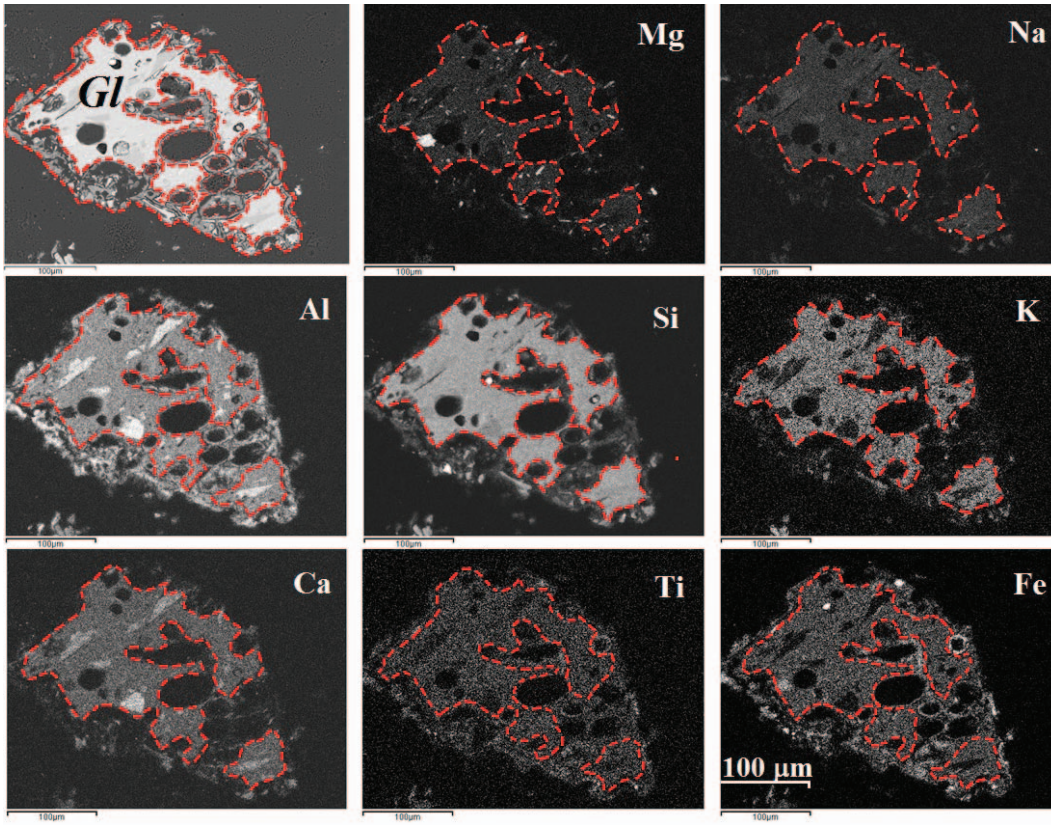

FIG. 2. Backscatter SEM images of a vesicular glass particle and accompanying element distribution maps derived from EPMA data. *Gl*, volcanic glass particle with vesicules; dotted line identifies the boundary between volcanic glass and area where it has altered to allophane. The element distribution images of Mg, Na, K and Ca indicate that these elements are absent or occurring in very low concentrations in this alteration zone; this suggests leaching from the glass during the alteration process. The element distribution images of Al, Ti and Fe suggest that they have been enhanced in this alteration zone.

weathering (Henmi & Parfitt, 1980). The completely altered soft zone is filled with spherical bodies (Fig. 5b) and these are characteristic of opaline silica (Pollard & Weaver, 1973). These particles differ from glass fragments which are more angular (Fig. 6). The elemental compositions of the opaline

TABLE 5. Chemical composition (atomic wt.%) of minerals (*A1-A7*, areas where analyses were made; *A1*, *A2* represent allophone; *A3–A5*, opaline silica; *A6*, *A7*, volcanic glass).

Area no.	O	Na	Mg	Al	Si	Cl	K	Ca	Ti	Cr	Fe	Total
A1	52.63	0.21	0.66	24.18	15.18	–	–	4.37	–	–	2.77	100
A2	49.95	–	0.25	26.71	18.85	–	–	1.36	0.25	–	2.63	100
A3	57.86	0.10	1.07	9.97	29.42	–	0.08	0.05	0.27	0.07	1.11	100
A4	61.02	1.57	0.25	5.64	27.96	0.06	1.71	0.79	0.13	0.03	0.82	100
A5	59.45	1.3	0.32	7.38	25.26	0.05	0.03	0.04	0.21	0.12	5.83	100
A6	59.14	0.95	0.22	5.84	30.22	0.08	1.72	0.85	0.14	0.06	0.78	100
A7	57.72	1.48	0.23	6.29	30.32	0.08	1.8	0.94	0.17	0.07	0.90	100

https://doi.org/10.1180/claymin.2014.049.2.04 Published online by Cambridge University Press

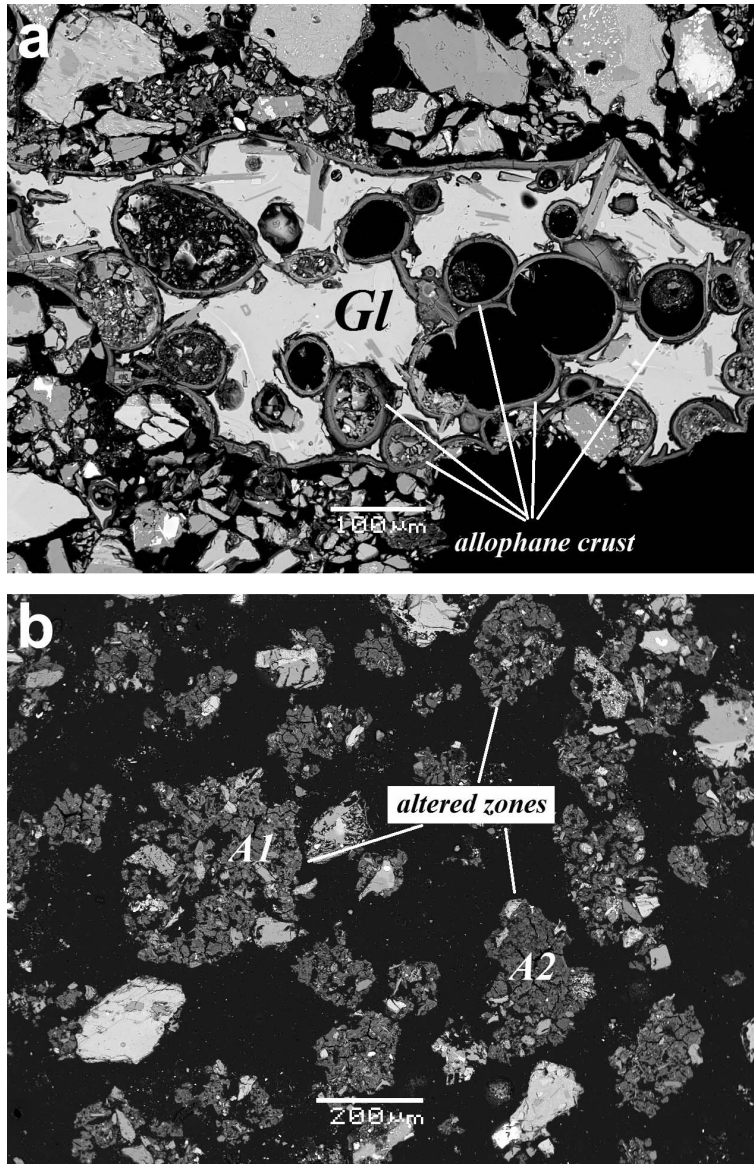

FIG. 3. (a) Backscatter SEM image showing extensive allophane alteration crusts in and around a vesicular glass particle (arrowed) in sample *5*; *Gl*, volcanic glass. (b) Backscatter SEM image showing unconsolidated ash (sample *18*) in which leaching and desilicification of glass has resulted in very fine-grained aggregates of allophane (zone *A1* and *A2*).

silica and volcanic glass are shown in Table 5 with the analysed areas marked on the micrographs.

Gaillou *et al.* (2008) has emphasized that opal is not a pure form of silica as it contains water as a component, and various impurities and trace elements can also enter its structure. The most common impurity is aluminium, which substitutes for silicon (Bartoli *et al.*, 1990). The investigation of Australian opals, representing 95% of world production (Horton, 2002), as well as opals from USA and Brazil, shows that the 'impurities' (i.e. elements present at concentration above 500 ppm)

https://doi.org/10.1180/claymin.2014.049.2.04 Published online by Cambridge University Press

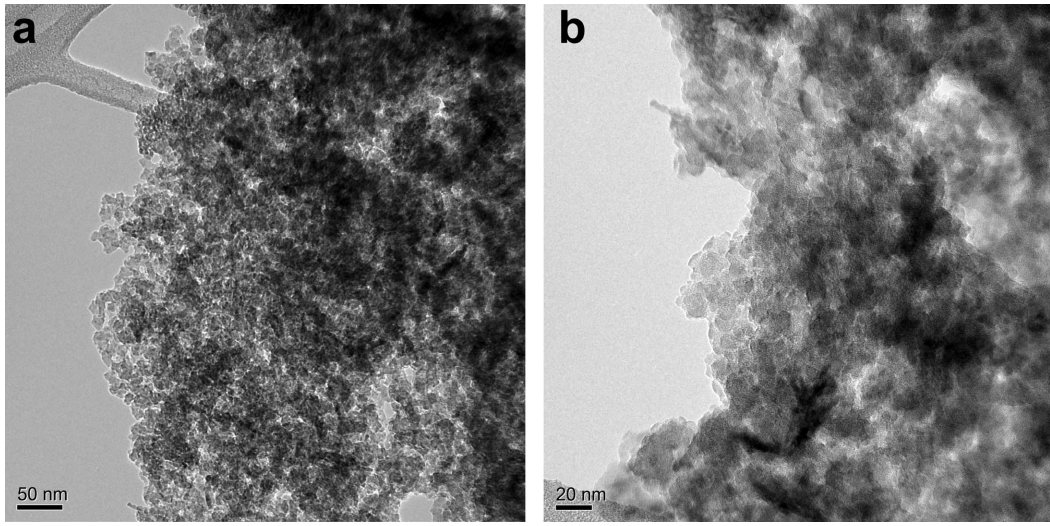

FIG. 4. (a,b) Transmission electron micrographs of opaline silica in sample *24*.

include Al, Ca, K, Mg, Fe and Na. Elements at concentrations below 500 ppm are referred to as 'trace elements'. These are mainly Ba, Sr, Rb, Mn and Ti (Bayliss & Males, 1965; Bartoli *et al.*, 1990; McOrist *et al.*, 1994; McOrist & Smallwood, 1995, 1997). Some studies link the chemistry of opals to that of the host rock, even if modified by weathering processes (Gaillou *et al.*, 2008).

INTERPRETATION

Henmi & Parfitt (1980) concluded that opaline silica is characteristic of the early stages of weathering of volcanic ash in the humid temperate climatic zone. Our observations of volcanic ash from Kamchatka show that cold humid climates and permafrost can preserve opaline silica.

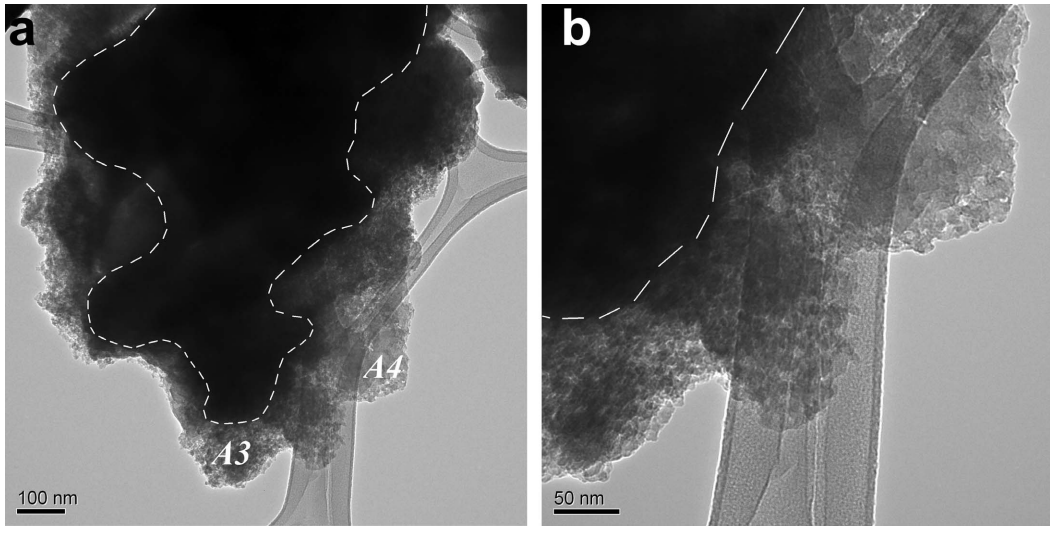

FIG. 5. (a,b) Transmission electron micrographs showing a glass particle in sample *24* with an outer zone of opaline silica; the boundary between the altered and unaltered zones is indicated by the dotted line; the locations of analyses *A3* and *A4* (Table 5*)* are shown.

https://doi.org/10.1180/claymin.2014.049.2.04 Published online by Cambridge University Press

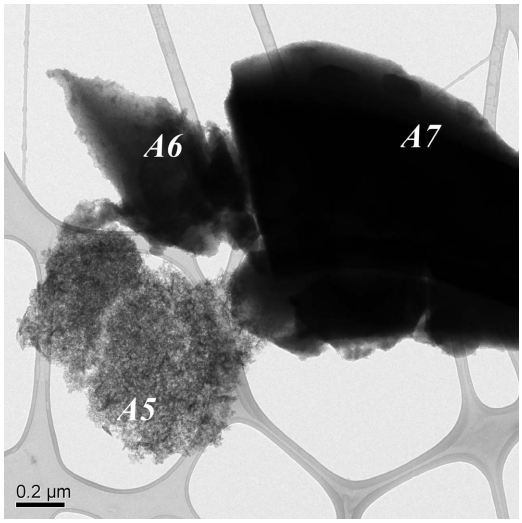

FIG. 6. Transmission electron micrograph of opaline silica (*A5*) and glass particles (*A6*, *A7*).

Figure 7 is a crossplot of the total and adsorbed water contents (W_{term} and W_g) of volcanic ash samples (Table 6) *vs*. sample age. This shows a correlation between the total mass loss of water (W_{term}) in the ashes and the age and chemical composition of the glass contained in those ashes. Ashes containing glass with andesitic composition have twice as much water as ashes of a similar age with glass of rhyolite composition (Fig. 7a). Similar correlation between the age of the ash and the amount of adsorbed water (W_g) is evident when the samples were dried (Table 6; Fig. 7b). The water content of the ashes containing opal is considerably lower than for those containing allophane. This suggests a higher rate of transformation of the ashes containing allophane.

Samples *9* and *15*, both containing rhyolitic glass and of similar age (Table 6), contain opal but display considerable differences in the total water content of their host ashes (Table 6). This might be explained by the different rates of alteration. Sample *15* comes from the forest zone at an altitude of 290 m, whereas sample *9* is from the tundra zone at 695 m. The higher water content of the ash in sample *15* could reflect the enhanced weathering associated with the higher average temperature at 290 m.

Unfrozen water content

The unfrozen water content of soils under permafrost conditions is an essential part of their thermo-physical characteristics. It alters the thermal conductivity and heat capacity of volcanic ashes and soils and the rate at which volcanic glass and minerals may weather under permafrost conditions (Motenko & Kuznetsova, 2009a,b; Kuznetsova *et al.*, 2011).

Figure 8 is a crossplot showing the unfrozen water content, W_w , and temperature for samples containing either allophane or opal. For temperature below −3ºC (where the variation of unfrozen water content is insignificant) the value of W_w changes from 2 to 13% for ashes containing allophane (area 1) and from 0 to 3% for ashes containing opal (area 2).

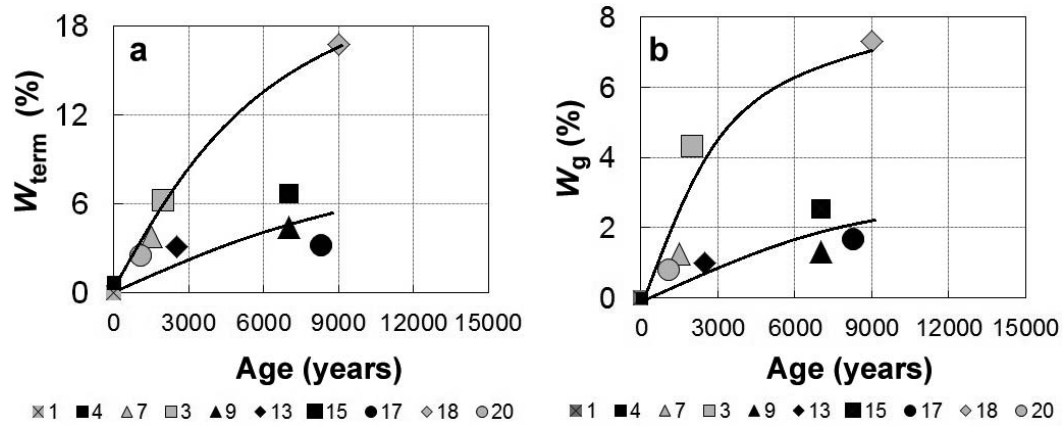

FIG. 7. (a,b) The relationship between the total and adsorbed water contents of basaltic, andesitic and rhyolitic ashes as a function of age; the numbers under the diagrams correspond to sample numbers.

https://doi.org/10.1180/claymin.2014.049.2.04 Published online by Cambridge University Press

TABLE 6. Relationships between water contents, age, altitude and glass compositions of ash samples of different compositions.

Sample no.	W_{term}* (%)	Age (years)	Attitude (m)	Mineral composition	Glass composition	W_g* (%)
8	0	35	1330	Waterless allophane	Basaltic	0
20	2.5	950–1400	800	Allophane		0.79
7	3.8	1500	1630	Allophane		1.24
3	6.2	1500	1630	Allophane	Andesitic	4.3
18	16.8	8500–9000	290	Allophane		7.3
4	0.6	35	1000	Waterless opal	Rhyolitic	0
13	3.1	2500	746	Opal		1
9	4.4	6850	695	Opal		1.32
15	6.7	6850	290	Opal		2.52
17	3.2	8300	290	Opal		1.67
24	6.1	Q_1^2	129	Opal		0.93

* Note: W_{term}, water from thermal method representing amount of structural and absorbed water together, wt. %; W_g , absorbed water (in relation to the weight of dry soil), wt.%.

According to many investigations (e.g. Henmi & Wada, 1976; Theng *et al.*, 1982), allophane consists of hollow spheres with an outer diameter of about 4–5 nm, with defects in the wall texture which consequently form micro-pores (0.3–2.0 nm) and with an active specific surface area of 800 m^2/g. The unfrozen water retention capacity of the ashes containing allophane could be related to the presence of these very small pores and the extensive active specific surface areas. This is in contrast to opals with a somewhat similar basic physical structure of more or less close-packed silica spheres of amorphous silica. However their active specific surface area is much lower (<0.5 m^2/g; Jones & Segnit, 1969), which may be one of the explanations of the smaller amount of unfrozen water content in samples with opal.

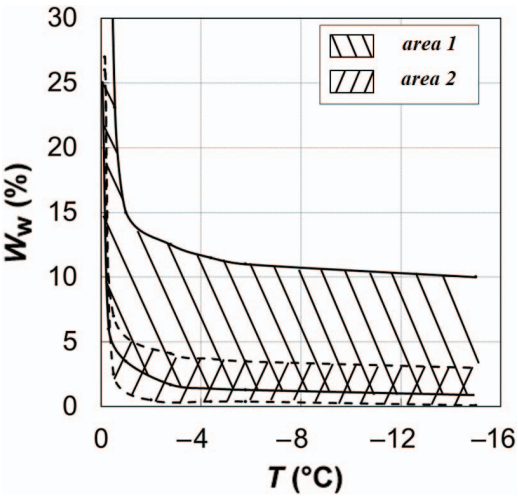

FIG. 8. Cross plot of the unfrozen water content W_w and temperature for the studied samples. Area 1, ash samples containing allophone; Area 2, ash samples containing opal.

Sample *24* is a rhyolitic ash from the exposure Krutoy on the bank of the Kamchata River at an elevation of 130 m. The ash has a high-salinity pore water content (see above) and is considerably older than the other samples (upper Lower Pleistocene cf. Holocene) we have investigated. The high salinity is thought to be related to the incorporation of sulfates (and sometimes chlorides) during eruptions and not to post-magmatic alteration (Girina, 1998). The sample is exceptional, as it is sandwiched between two layers of unsalted clayey loam (Fig. 9a, samples *24′* and *24″*). In spite of its age the IR and TEM analyses indicated only the presence of opaline silica and no halloysite or other clay minerals from the alteration of the volcanic glass. The unfrozen water content is high, nearly 27% in the temperature range below the phase transition of water (< –3ºC), whereas in the overlying and underlying samples (*24′*, *24″*) W_w is only 2–3%. This exceptional high value may reflect the high salinity of sample *24*. Figure 9b shows the unfrozen water content W_w *vs.* the negative temperature for these three samples. The

https://doi.org/10.1180/claymin.2014.049.2.04 Published online by Cambridge University Press

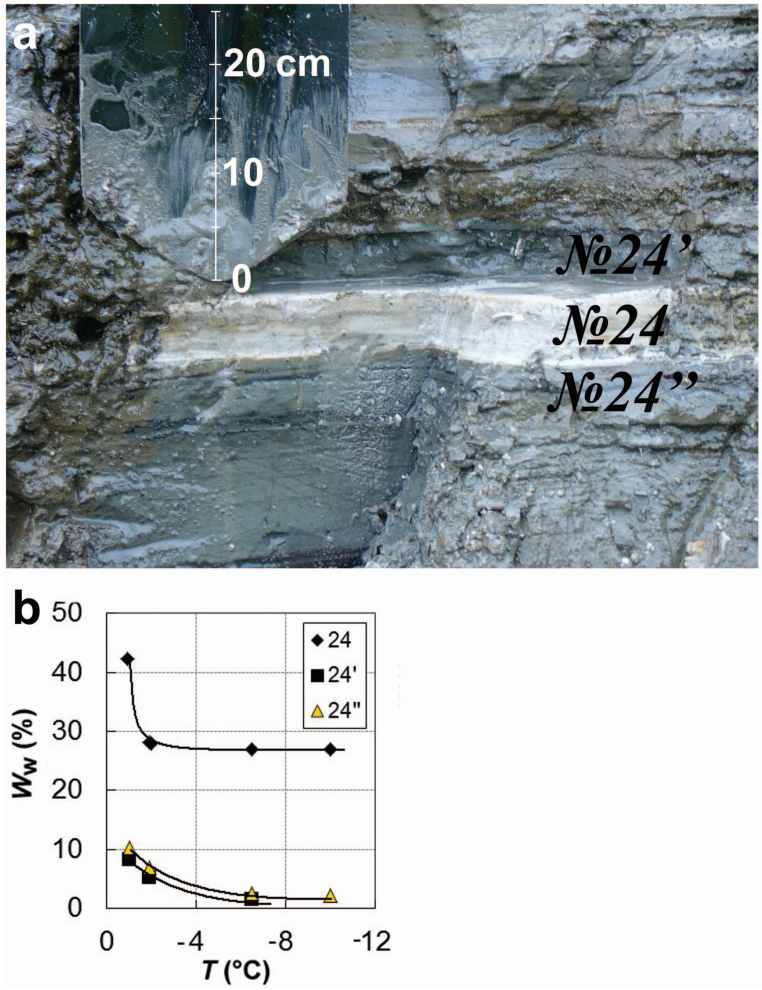

FIG. 9. (a) Soil section showing ash layer (*24*) which is sandwiched between two layers of clayey loam (*24′* and *24″*). (b) Cross plot of the unfrozen water content and temperature for saline (*24*) and non-saline samples (*24′* and *24″*).

limited alteration of sample *24* suggests its preservation by palaeopermafrost conditions persisting in the profile in spite of its low altitude (130 m).

Figure 10 shows the relationship between the unfrozen water content (W_w) and the age of all the investigated samples. There are four groups depending on sampling altitude: 1600 m, 1000–1300 m, 700–800 m, and 290 m and below. These are discussed below.

Group 1. The samples *1*, *3*, *5* and *7* are of similar age, ~1500 years old. They are from the tundra zone on the Tolbachinskiy Pass at an altitude of 1600 m where permafrost is widespread. Samples *1*, *3* and *5* were collected from the seasonal melting layer (the active layer) at the top of the soil, which is the site of cryogenic weathering. These soils experienced radical temperature fluctuations with repeated freezing and thawing cycles which are a controlling factor in the composition and structural changes taking place in this layer. All the samples contain andesitic glass and are associated with allophane but contain varying amounts of unfrozen water. These samples show differences in their colour and granulometric composition. Samples *1*, *5* and *7* are brown in colour and have a similar grain size, whereas sample *3* is bright orange and is of finer

https://doi.org/10.1180/claymin.2014.049.2.04 Published online by Cambridge University Press

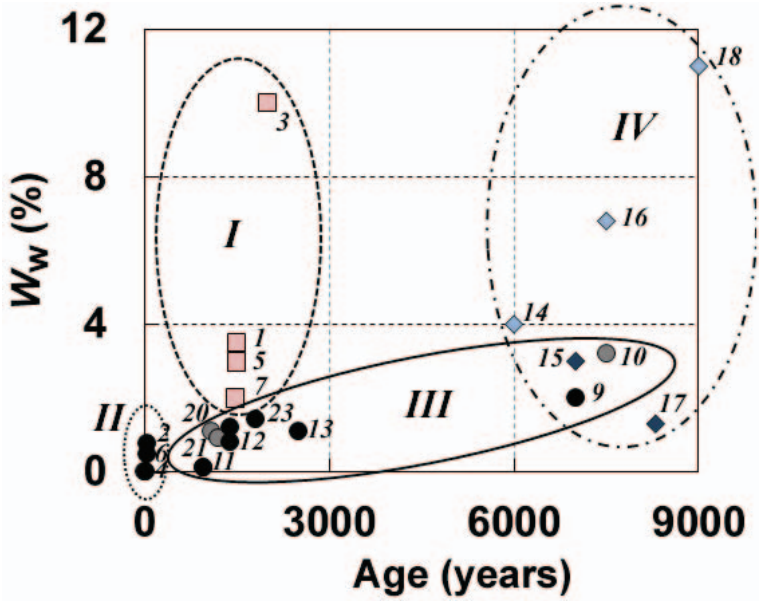

FIG. 10. Cross plot of the unfrozen water content and sample age showing their interdependence. Roman numerals indicate the grouping of samples based on their altitudes: *I*, 1600 m; *II*, 1000–1300 m; *III*, 700–800 m; *IV*, 290 m.

grain size. The active freeze-thaw boundary at the time of observation was along a bright yellow, very fine grained ash layer. Drawing an analogy between the ash from this existing active boundary and sample *3*, we conclude that an earlier freeze-thaw boundary was situated higher in the profile along the horizon where sample *3* was collected.

Two extreme weathering situations occur in this area; they are represented by two samples. Sample *7* is from a borehole in the permafrost. It has been permanently in the frozen state and was never involved in the active layer. Sample *3* is from a freeze-thaw boundary. Samples *1* and *5* were collected from the upper part of the active layer where there is no repeated temperature transition during the warm season. The highest content of unfrozen water was found in sample *3*, and the smallest in samples *1* and *5*, with a difference of 8% between them.

Group II. This group of samples (*2*, *4*, *6* and *8*) are from the tundra zone at an altitude of 1000–1300 m in the proximity of the Large Fissure Eruption at Tolbachik and near the Kamen volcano area. Their age is nearly 35 years. The glass from samples *2, 4* and *6* is of rhyolitic composition and is associated with opal; sample *8* has a basaltic composition (Girina, 1998) and is associated with allophane. The content of unfrozen water is low (0–0.5%).

Group III. These samples (*9–13*, *19–21* and *23*) are from an altitude of 700–800 m from an area within the tundra zone with seasonal permafrost. The glass composition of samples *9*, *11–13*, *19* and *23* is rhyolitic and is associated with opal, sample *10* is andesitic and is associated with allophane, and samples *20* and *21* are basaltic and are associated with allophane (see Table 3, Braitseva *et al.*, 1997; Ponomareva *et al.*, 2007a,b). There is some correlation between the unfrozen water content, sample age and the presence of allophane or opal. The unfrozen water contents tend to be higher in the older samples or those containing allophane.

Group IV. The samples *14–18* were from an altitude of 290 m. There is only seasonal freezing at this altitude, but it is already within the upper part of the forest zone.

Samples *15* and *17* have rhyolitic glass and contain opal; samples *14*, *16* and *18* have andesitic glass and contain allophane. The unfrozen water content is higher in samples with allophane than those with opal.

https://doi.org/10.1180/claymin.2014.049.2.04 Published online by Cambridge University Press

Thermal properties

Measurements of thermal conductivity were made for volcanic ashes of different age, mineralogy, chemistry and grain size, and have been reported in previous publications (Motenko *et al.*, 2008; Kuznetsova & Motenko, 2011a,b).

These data show that when the density (ρ_d) and moisture content (W) of the ash samples change from 0.7 to 1.65 g/cm^3 and from 10 to 80% respectively the thermal conductivity (λ) increases from 0.37 to 1.0 W/(m·K) in the thawed state and from 0.41 to 1.27 W/(m·K) in the frozen state. All physical properties of frozen grounds are controlled by unfrozen water (W_w) and ice content ($W-W_w$), because the thermal conductivity (λ) of ice (2.2 W/(m·K)) is much greater than that of water (0.56 W/(m·K)). The influence of the presence of allophane on $W_w/(W-W_w)$ ratio and therefore on the thermal conductivity in frozen volcanic ashes is seen in Fig. 11. This shows the thermal conductivity of frozen ashes versus the unfrozen water and ice ratio at temperatures below −3ºC. In the ashes containing opal (lines *I* and *II*), there is little unfrozen water with the combined unfrozen water and ice content ratio varying from 0 to 0.08. On line *I* there are data for samples *2*, *4* and *19* in which there is practically no unfrozen water; on line *II* there are data for samples *6*, *9*, *12* and *17*, with values of W_w ranging from 0.5 to 1.1%.

In the ashes containing allophane (lines *III*, *IV* and *V*) with unfrozen water contents ranging from 2 to 11%, the ratio $W_w/(W-W_w)$ varies from 0.08 to 0.58. The line *III* averages data for samples *10*, *14*, *15*, *20* and *21*, where the unfrozen water content is 0.8−3%, The line *IV* for samples *1*, *5* and *7* has values of 2−4%, and line *V* for samples *3* and *18* has an unfrozen water content of 10−11%.

A small change in the water to ice ratio, for example from 0.02 to 0.04 in the ashes containing opal, causes a decrease of thermal conductivity by a factor of 2. For ashes containing allophane there is a change in thermal conductivity by a factor of 3 due to a greater variation in this ratio from 0.19 to 0.58.

CONCLUSIONS

1. The mineralogical analysis showed that allophane was found in ash samples with andesitic and basaltic glass, and opal in samples with rhyolitic glass.

2. Even in the oldest ash deposits such as an example from the second half of early Pleistocene

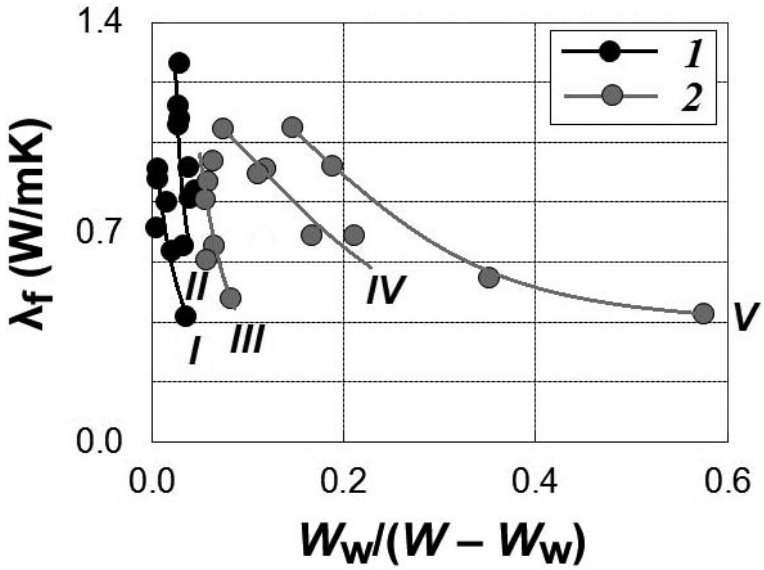

FIG. 11. Cross plot of thermal conductivity and the unfrozen water (W_w) and ice ($W-W_w$) ratio under the temperature of −10ºC. Lines show the data for: (1) (*I* and *II*), ash samples containing opal; and (2) (*III*, *IV* and *V*), ash samples containing allophane with different unfrozen water content: *I*, W_w <0.5%; *II*, 0.5 <W_w <1.1%; *III*, 0.8 <W_w <3%; *IV*, 2 <W_w <4%; *V*, W_w =10−11%.

https://doi.org/10.1180/claymin.2014.049.2.04 Published online by Cambridge University Press

(Q_I^2) there was no evidence of halloysite or other clays which could be linked with palaeopermafrost conditions.

3. The amount of structural and adsorbed water depends on sample age and glass composition. The content is higher in the samples with basaltic and andesitic glass containing allophane, and lower in the samples with rhyolitic glass and opal.

4. The content of unfrozen water is higher in volcanic ashes containing allophane than in those containing opal.

5. The highest proportion of unfrozen water occurred in an ash with high soil water salinity.

6. There are four distinct groups of ash samples related to altitude that can be distinguished by their volcanic glass alteration and unfrozen water contents. There are two high-altitude groups above 1600 m and 1100 m asl, an intermediate region consisting of samples from 700–800 m, and a low altitude region with samples from below 290 m. The first three regions are in tundra zones and the last one in the forest zone. The greatest alteration takes place in the high-altitude region in samples from the seasonally melting layer, especially in the interface between frozen and thawed grounds.

7. Thermal conductivity in frozen soils depends on the unfrozen water and ice content and the mineralogical composition of the samples. Even a small change in the water to ice ratio in the ashes containing opal causes a decrease in thermal conductivity by a factor of 2. For ashes containing allophane, this change is by a factor of 3, reflecting the greater variation in the water to ice ratios of these ashes.

ACKNOWLEDGMENTS

Experimental work was cattied out at the Department of Geocryology of Lomonosov Moscow State University as a part of the first author's PhD work. We wish to thank the following: S.W. Danielsen from SINTEF Building and Infrastructure for help in preparing the manuscript; J. Walmsley from SINTEF Materials and Chemistry for TEM analysis; M.F. Vigasina and L.V. Melchakova from Lomonosov Moscow State University for IR and thermal studies; Muravyev Ya.D., Deputy Director in Volcanology and Seismology Institute of the RAS FEB, for the field works in Kamchatka in 2009-2011, and for valuable consultations; C.V. Jeans, H.F.Shaw and M.J.Wilson for their constructive comments and editorial help.

REFERENCES

Abramov A., Gruber S. & Gilichinsky D. (2008) Mountain permafrost on active volcanoes: field data and statistical mapping, Kluchevskaya volcano group, Kamchatka, Russia. *Permafrost and Periglacial Processes*, **19**, 261–277 (in Russian).

Bartoli F., Bittencourt Rosa D., Doirisse M., Meyer R., Philippy R. & Samana J.C. (1990) Role of aluminium in the structure of Brasilian opals. *European Journal of Mineralogy*, **2**, 611–619.

Bayliss P. & Males P.A. (1965) The mineralogical similarity of precious and common opal from Australia. *Mineralogical Magazine*, **35**, 429–431.

Bazanova L.I., Braitseva O.A., Dirksen O.V., Sulerzhitskiy L.D. & Dankhara T. (2005) Ash falls of major Holocene eruptions at the Ust-Bolsheretsk – Petropavlovsk-Kamchatsky traverse: sources, chronology, frequency. *Volcanology and Seismology*, **6**, 30–46.

Braitseva O.A., Melekestsev I.V., Evteeva I.S. & Lupikina E.G. (1968) *Stratigraphy of Quaternary Sediments and Glaciations of Kamchatka.* Nauka, Moscow (in Russian).

Braitseva O.A., Melekestsev I.V., Ponomareva V.V. & Sulerzhitsky L.D. (1995) The ages of calderas, large explosive craters and active volcanoes in the Kuril–Kamchatka region, Russia. *Bulletin of Volcanology*, **57**, 383–402.

Braitseva O.A., Ponomareva V.V., Sulerzhitsky L.D. & Melekestsev I.V. (1997) Holocene Key-Marker Tephra Layers in Kamchatka, Russia. *Quaternary Research*, **7**, 125–139.

Deveson B. (2004) The origin of precious opal: a new model. *Australian Gemmologist*, **22**, 50–58.

Fedotov S.A. & Markhinin Y.K. (1983) *The Great Tolbachik Fissure Eruption: Geological and Geophysical Data, 1975–1976.* Cambridge University Press.

Gaillou E., Delaunay A., Rondeau B., Bouhnik-le-Coz M., Fritsch E., Cornen G. & Monnier C. (2008) The geochemistry of gem opals as evidence of their origin. *Ore Geology Reviews*, **34**, 1–2, 113–126.

Girina O.A. (1998) *Pyroclastic Deposits of Recent Eruptions of Andesitic Volcanoes of Kamchatka and their Engineering and Geological Features*. Dalnauka, Vladivostok (in Russian).

Henmi T. & Parfitt R.L. (1980) Laminar opaline silica from some volcanic ash soils in New Zealand. *Clays and Clay Minerals*, **28**, 57–60.

Henmi T. & Wada K. (1976) Morphology and composition of allophane. *American Mineralogist*, **61**, 379–390.

Horton D. (2002) Australian sedimentary opal: why is Australia unique? *The Australian Gemologist*, **21**, 8.

Jeffery P.G. & Hutchison D. (1983) *Chemical Methods of Rock Analysis*, 3rd edition. Pergamon Press,

Oxford, UK.
Jones J.B. & Segnit E.R. (1969) Water in sphere-type opal. *Mineralogical Magazine*, **37**, 357–361.
Kalachev V.Ya., Volovik M.E. & Ladygin V.M. (1997) Express method of soils particle density determination. *Vestnik MSU Geology*, **2**, 51–56 (in Russian).
Kiryanov V.U. (1981) About the possibility of correlation of ash horizons in the Pleistocene deposits of the Central Kamchatka Depression. *Volcanology and Seismology*, **6**, 30–38.
Kuznetsova E. & Motenko R. (2011a) The influence of allophane appearance on the thermal conductivity of frozen volcanic ashes (Kamchatka). Pp. 95–96 in: *Proceeding of Euroclay 2011 Conference*. Antalya, Turkey.
Kuznetsova E.P. & Motenko R.G. (2011b) Heat-conducting characteristics of the Kamchatka volcanic ash. Pp. 91–97 in: *Proceedings of IV Conference of Geocryologist of Russia*, **1**. MGU, Moscow.
Kuznetsova E. & Motenko R. (2012) Impact of mineral composition on heat-conducting properties of frozen volcanic ashes in Kamchatka. Pp. 225–230 in: *Proceedings of 10th International Conference on Permafrost (TICOP 2012)*, **2**.
Kuznetsova E.P., Motenko R.G., Vigasina M.F. & Melchakova L.V. (2011) Unfrozen water research in Kamchatka volcanic ash. *Vestnik MGU Geology*, **1**, 62–67.
Lowe D.J. (1986) Controls on the rates of weathering and clay mineral genesis in airfall tephras: a review and New Zealand case study. Pp. 265–330 in: *Rates of Chemical Weathering of Rocks and Minerals* (S.M. Colman & D.P. Dethier, editors). Academic Press, Orlando.
McOrist G.D. & Smallwood A. (1995) Trace elements in colored opals using neutron activation analysis. *Journal of Radioanalytical and Nuclear Chemistry*, **198**, 499–510.
McOrist G.D. & Smallwood A. (1997) Trace elements in precious and common opals using neutron activation analysis. *Journal of Radioanalytical and Nuclear Chemistry*, **223**, 9–15.
McOrist G.D., Smallwood A. & Fardy J.J. (1994) Trace elements in Australian opals using neutron activation analysis. *Journal of Radioanalytical and Nuclear Chemistry*, **185**, 293–303.
Melekestsev I.V., Kraevaya T.S. & Braytseva O.A. (1969) Soil-pyroclastic cover and its value for tephrochronology in Kamchatka. Pp. 61–71 in: *Kamchatka Volcanic Facies*. Nauka, Moscow (in Russian).
Motenko R.G. & Kuznetsova E.P. (2009a) Formation of phase composition of water in the frozen volcanic ashes (Kluchevskaya volcano group, Kamchatka). Pp. 518–521 in: *Proceeding of the 8th International Symposium on Permafrost Engineering.* China.
Motenko R.G. & Kuznetsova E.P. (2009b) Estimate of unfrozen water content for frozen volcanic ashes of different ages. Pp. 26–27 in: *Proceeding of Futuroclays Meeting.* Newcastle, England.
Motenko R.G, Tikhonova (Kuznetsova) E.P. & Abramov A.A. (2008) Experimental study of thermal properties for frozen pyroclastic volcanic deposits (Kamchatka, Kluchevskaya volcano group). Pp. 1251–1254 in: *Proceeding of the 9th International Conference on Permafrost*. Fairbanks, Alaska, USA.
Muravyev Y.D. (1999) Present-day glaciation in Kamchatka – distribution of glaciers and snow. Pp. 1–7 in: *Cryospheric Studies in Kamchatka II*. Hokkaido University, Sapporo.
Nagasawa K. (1978) Weathering of volcanic ash and other pyroclastic materials. Pp. 105–125 in: *Clays and Clay Minerals in Japan* (T. Sudo & S. Shimada, editors). Kondansha, Tokyo/Elsevier, Amsterdam.
Nanzyo M. (2002) Unique properties of volcanic ash soils. *Global Environmental Research*, **6**, 99–112.
Parfitt R.L., Russel M. & Orbell G.E. (1983) Weathering sequence of soils from volcanic ash involving allophane and halloysite. *Geoderma*, **41**, 223–241.
Parfitt R.L. & Wilson A.D. (1985) Estimation of allophane and halloysite in three sequences of volcanic soils, New Zealand. Pp. 1–8 in: *Volcanic Soils, Weathering and Landscape Relationships of Soils on Tephra and Basalt* (E. Fernandez Caldas & D.H. Yaalon, editors). Catena Verlag, Cremlingen.
Peng Wenshi (1982) *IR Spectra of Minerals.* Science, Bejing.
Platunov E.S. (1972) *Thermophysical Measurements in a Monotonic Cycle*. Energy, Moscow (in Russian).
Plyusnina I.I. (1977) *Infrared Mineral Spectra*. MSU, Moscow.
Pollard & Weaver (1973) Opaline spheres: loosely packed aggregates from silica nodule in diatomaceous Miocene fuller's earth. *Journal of Sedimentary Petrology*, **43**, 1072–1076.
Ponomareva V.V., Churikova T.G., Melekestsev I.V., Braitseva O.A., Pevzner M.M. & Sulerzhitsky L.D. (2007a) Late Pleistocene-Holocene volcanism on the Kamchatka Peninsula, northwest Pacific region. Pp. 165–198 in: *Volcanism and Subduction: The Kamchatka Region* (J. Eichelberger, P. Izbekov, N. Ruppert, J. Lees & E. Gordeev, editors). *American Geophysical Union Geophysical Monograph Series*, **172**.
Ponomareva V.V., Kyle P.R., Pevzner M.M., Sulerzhitsky L.D. & Hartman M. (2007b) Holocene eruptive history of Shiveluch volcano. Kamchatka Peninsula. Pp. 263–282 in: *Volcanism and Subduction: The Kamchatka Region* (J. Eichelberger, P. Izbekov, N. Ruppert, J. Lees & E. Gordeev, editors). *American Geophysical Union Geophysical Monograph Series*, **172**
Theng B.K.G., Russell M., Churchman G.J. & Parfitt R.L. (1982) Surface properties of allophone, halloy-

https://doi.org/10.1180/claymin.2014.049.2.04 Published online by Cambridge University Press

site and imogolite. *Clay and Clay Minerals*, **30**, 143–149.

Topor N.D., Ogorodova L.P. & Melchakova L.V. (1987) *Thermal Analysis of Minerals and Inorganic Compounds.* MSU, Moscow.

Wada K. (1989) Allophane and imogolite. Pp: 1051–1087 in: *Minerals in Soil Environments* (J.B. Dixon & S.B. Weed, editors). Soil Science Society of America, Madison, WI, USA, **21**.

Wada S-I. & Wada K. (1977) Density and structure of allophane. *Clay Minerals*, **12**, 289–298.

Yamada I. & Shoji S. (1975) Relationships between particle size and mineral composition of volcanic ashes. *Tohoku Journal of Agricultural Research*, **26**, 7–10.

Yamada I. & Shoji S. (1983) Properties of volcanic glasses and relationships between the properties of tephra and volcanic zones. *Japanese Journal of Soil Science and Plant Nutrition*, **47**, 755–765.

Zakharikhina L. (2009) *Peculiarities of soil formation and soil chemistry under active volcanism conditions (on the example of Kamchatka).* Candidate dissertation. Novosibirsk, Russia (in Russian).

https://doi.org/10.1180/claymin.2014.049.2.04 Published online by Cambridge University Press